



## OPEN ACCESS

EDITED BY  
Zheng Xiang,  
Liaoning University, China

REVIEWED BY  
Qiang Meng,  
Dalian Medical University, China  
Haibo Xu,  
Chengdu University of Traditional  
Chinese Medicine, China

\*CORRESPONDENCE  
Yu-hui Yan,  
ctyanyh@163.com

SPECIALTY SECTION  
This article was submitted to  
Ethnopharmacology,  
a section of the journal  
Frontiers in Pharmacology

RECEIVED 29 September 2022  
ACCEPTED 18 October 2022  
PUBLISHED 26 October 2022

CITATION  
Yan Y-h, Huang Z-h, Xiong Q-p,  
Song Y-w, Li S-y, Yang B-w, Sun L,  
Zhang M-y and Ji Y (2022), Effects of  
*Broussonetia papyrifera* (L.) L'Hér. ex  
Vent. fruits water extract on  
hippocampal neurogenesis in the  
treatment of APP/PS1 transgenic mice.  
*Front. Pharmacol.* 13:1056614.  
doi: 10.3389/fphar.2022.1056614

COPYRIGHT  
© 2022 Yan, Huang, Xiong, Song, Li,  
Yang, Sun, Zhang and Ji. This is an open-  
access article distributed under the  
terms of the [Creative Commons  
Attribution License \(CC BY\)](https://creativecommons.org/licenses/by/4.0/). The use,  
distribution or reproduction in other  
forums is permitted, provided the  
original author(s) and the copyright  
owner(s) are credited and that the  
original publication in this journal is  
cited, in accordance with accepted  
academic practice. No use, distribution  
or reproduction is permitted which does  
not comply with these terms.

# Effects of *Broussonetia papyrifera* (L.) L'Hér. ex Vent. fruits water extract on hippocampal neurogenesis in the treatment of APP/PS1 transgenic mice

Yu-hui Yan<sup>1\*</sup>, Zi-han Huang<sup>1,2</sup>, Qing-ping Xiong<sup>3</sup>,  
Yue-wen Song<sup>1</sup>, Si-yang Li<sup>1</sup>, Bao-wei Yang<sup>1</sup>, Lan Sun<sup>1</sup>,  
Meng-yuan Zhang<sup>1</sup> and Yu Ji<sup>1</sup>

<sup>1</sup>School of Pharmacy, Jiangsu Food & Pharmaceutical Science College, Huai'an, Jiangsu, China,  
<sup>2</sup>School of Food Science and Engineering, Jiangsu Ocean University, Lianyungang, Jiangsu, China,  
<sup>3</sup>Jiangsu Key Laboratory of Regional Resource Exploitation and Medicinal Research, Huaiyin Institute  
of Technology, Huai'an, Jiangsu, China

**Background:** Adult neurogenesis plays an important role in repairing damaged neurons and improving cognitive impairment in Alzheimer's disease (AD). *B. Papyrifera* (L.) L'Hér. ex Vent. fruits (BL), a traditional Chinese medicine for tonifying the kidney, has been reported to improve cognitive function in AD mice, but the underlying mechanisms have not been clearly illuminated. This study aimed to provide an overview of the differential compounds in the brain of APP/PS1 mice after BL water extract (BLWE) treatment through metabolomics technology and to elucidate whether the therapeutic effect and mechanism are through the enhancement of neurogenesis.

**Methods:** APP/PS1 transgenic mice were treated with different doses of BLWE. After 6 weeks of intragastric injection, the therapeutic effects of BLWE on APP/PS1 transgenic mice were determined by the Morris water maze test, immunohistochemistry, hematoxylin & eosin and Nissl staining, enzyme-linked immunosorbent assay and terminal deoxynucleotidyl transferase dUTP nick end labeling staining. Subsequently, metabolomics technology was used to analyze the regulatory effect of BLWE on differential compounds in the brain of APP/PS1 mice, and on this basis, its molecular mechanism of BLWE was screened. Finally, the protein expression of the Wnt/ $\beta$ -catenin signaling pathway was detected by Western blotting.

**Results:** After BLWE treatment, the learning and memory function of APP/PS1 mice were significantly improved, which was related to the increase in the number of Nestin<sup>+</sup>/BrdU<sup>+</sup> and NeuN<sup>+</sup>/BrdU<sup>+</sup> cells, and the decrease in the number of apoptotic cells in the hippocampus. BLWE treatment could also up-regulate the expression of synapse-associated proteins. Moreover, BLWE could modulate endogenous metabolic compounds in the brains of AD mice, including N-acetyl-aspartate, glutamine, etc. Furthermore, BLWE inhibited

the phosphorylation of Tyr216-GSK-3 $\beta$  and  $\beta$ -catenin protein while increased CyclinD<sub>1</sub> protein expression.

**Conclusion:** We demonstrated that BLWE can enhance neural stem cells proliferation and improve neurogenesis, thereby efficiently repairing damaged neurons in the hippocampus and ameliorating cognitive impairment in APP/PS1 transgenic mice. The mechanism is at least partly through activating the Wnt/ $\beta$ -catenin signaling pathway.

#### KEYWORDS

*Broussonetia papyrifera* (L.) L'Hér. ex Vent. fruits water extract (BLWE), Alzheimer's disease, neurogenesis, metabolomics, wnt/ $\beta$ -catenin signaling pathway

## Introduction

Alzheimer's disease (AD) is a common neurodegenerative disorder that affects the elderly. As the population ages, the prevalence of AD is rising, which represents a substantial threat to the health of older people. Among the pathological characteristics of AD is the aberrant amyloid beta peptide (A $\beta$ ) deposition in the brain, which may promote neuroinflammatory responses, leading to a high number of synaptic losses and neuronal death in the brain. Consequently, AD patients will lose their capacities for learning and memorization (Golde et al., 2018; Uddin et al., 2020; de Almeida et al., 2022; Shakir and Dugger, 2022). Drugs continue to play a significant role in the treatment of AD, with acetylcholinesterase inhibitors and N-methyl-D-aspartate receptor antagonists being two of the most used types of medications for this condition (Liang et al., 2022). However, these medications may only alleviate the symptoms of certain patients but cannot effectively compensate the loss of neurons in the brain (Schott et al., 2019). Consequently, there is an urgent need for novel treatment strategies.

Neural stem cells (NSCs) are self-renewing cell populations that have the ability to differentiate into neurons, astrocytes, and oligodendrocytes (Jaberi et al., 2021). NSCs transplantation is regarded to be a successful treatment option for AD. However, the inflammatory microenvironment in the AD patients brains is not favorable to the survival of transplanted NSCs, therefore the therapeutic benefit is limited (Llorens-Bobadilla and Martin-Villalba, 2017). It has been hypothesized through previous research that the adult mammalian brain lacks regenerative repair capabilities. The following studies, however, demonstrate that neurogenesis does occur in the adult central nervous system (CNS), allowing for the treatment of CNS degenerative diseases and the repair of CNS injuries (Gage, 2019; Hanspal and Gillotin, 2022). Stimulating the proliferation of endogenous NSCs is considered as a practical way for CNS disease treatment, including AD and other neurodegenerative diseases. Certain traditional Chinese medicinal herbs and their extracts or active compounds have the abilities to modulate the biological characteristics of NSCs and enhance neurogenesis (Chen et al., 2019b). Kong et al. (2015) reported that osthole, an active compound derived from *Angelica*

*biserrata*, can promote neurogenesis in the hippocampus of APP/PS1 transgenic mice. This resulted in an improvement in the mice's cognitive performance. The active substance Astragaloside VI, derived from *Radix Astragalii*, promotes the proliferation of NSCs and neurogenesis in a model of transient cerebral ischemia injury, thereby improving the restoration of neurological function in rats with post-ischemic stroke (Chen et al., 2019a).

*Broussonetia papyrifera* (L.) L'Hér. ex Vent. fruits (BL) is a kind of Chinese herbal medicine distributed in most parts of China. Recent studies have revealed that BL extracts have a wide range of pharmacological effects, some of which include boosting the immune system, lowering blood lipids, anti-oxidation, and offering protection against drug-induced liver injury (Pang et al., 2014; Zhang et al., 2020). In addition, recent pharmacological studies have shown that BL extracts have neuroprotective actions on improving cognitive function in AD mouse model and chronic cerebral hypoperfusion rat model (Liu et al., 2020; Li Y. H. et al., 2021). However, it is unknown whether BL water extract (BLWE) can stimulate the growth of endogenous NSCs.

The proliferation, differentiation of NSCs, and neuronal apoptosis are closely related to the Wnt/ $\beta$ -catenin signaling pathway (Yu et al., 2017). Recent studies showed that the expression of glycogen synthase kinase-3 $\beta$  (GSK-3 $\beta$ ) and  $\beta$ -catenin, two key molecules of the Wnt/ $\beta$ -catenin signaling pathway, were shown to be significantly different in normal mice and AD model mice (Sun et al., 2019; Menet et al., 2020). However, it is unknown if BLWE could increase the proliferation of endogenous NSCs and whether the Wnt/ $\beta$ -catenin signaling pathway is involved in this process. In this study, we aimed to assess the effects of BLWE on the neurogenesis of AD mice and to investigate underlying mechanism.

## Materials and methods

### Animals, drug preparation, and administration

BL was purchased from Kangmei Pharmaceutical Co., Ltd. (Guangdong, China). The voucher specimens were identified by

Professor Tian-min Wang, who is working at Liaoning University of Traditional Chinese Medicine, then put in Jiangsu Food & Pharmaceutical Science College for storage (No. JSFPC20191207-01, Huai'an, China). BL (90 g) was soaked in deionized water (900 ml) for 1 h, then heated to boil at 100°C, and maintained in micro-boiling state for 1 h by a thermostat electric heating mantle (DZTW, Shanghai Lichen, China). The extracted solution was collected, and the dregs of a decoction was continued to be extracted twice according the same method, combine the three extracts to obtain the BLWE. After that, the BLWE was concentrated, freeze-dried, and its yielding capacity was calculated by three repeated experiments. The extraction yield of BL was calculated to be 8.48%. 5-Bromo-2-deoxyuridine (BrdU, Sigma Chemical Company, St. Louis, MO, United States) was prepared with deionized to a final concentration of 10 mg/mL and then deposited at 4°C.

APP<sub>swe</sub>/PS1<sub>ΔE9</sub> transgenic (Tg) mice were purchased from Beijing HPK Bioscience Co., Ltd. (Beijing, China), which can overexpress mutated human APP and PS1 (APP<sub>swe</sub>/PS1<sub>ΔE9</sub>) genes and simulate the pathological features of AD patients. Usually, cognitive impairment can be observed in 7-month-old Tg mice, and Aβ deposits can be detected in the hippocampus and cortex of 10-month-old Tg mice (Zhang et al., 2021). In this study, 9-month-old Tg mice were used and divided into model group, BLWE low dose (L-dose) group, and BLWE high dose (H-dose) group. The dose of mouse was converted according to the dose of human body, that is, 0.15g/kg for BLWE L-dose group and 0.30g/kg for BLWE H-dose group. We treat APP/PS1 mice according to the 'Guidelines for the Care and Use of Laboratory Animals published by the Shanghai Science and Technology Press of China in 2012. The BLWE groups received different doses of BLWE intragastric treatment once daily for 6 weeks. The model group was given an equal volume of deionized water for 6 weeks, and wild-type C57BL/6 mice at the same age were used as the control group. Three days before the end of the administration, mice were injected with BrdU (50 mg/kg, i. p.) twice a day to label proliferative cells.

## Morris water maze test

Six weeks after administration, the learning and memory abilities of mice were evaluated by the MWM test. The MWM includes a circular pool with a black inner wall, a diameter of 120 cm and a height of 60 cm, a camera, and automatic image acquisition and analysis system. The pool was divided into four quadrants in which a 10 cm diameter platform was placed as an escape platform. Add water (25°C) until the water surface is 2 cm higher than the platform. The swimming paths of mice were captured with the camera, and the images were collected and analysed to assess their spatial acquisition and memory abilities.

The operation details could be reviewed from our previous research (Yan et al., 2018).

## Immunohistochemistry

After the MWM experiment, the mice were anesthetized by i. p. with pentobarbital sodium (40 mg/kg), and fixed in the supine position. The brains were taken after cardiac perfusion, placed in the precooled paraformaldehyde solution, and fixed for 4–6 h. A rotary microtome (RM2235, Leica, Germany) was used to prepare paraffin sections (4 μm).

Sections were transparented twice in xylene solution for 15 min each time and then dehydrated by 70%, 80%, and 90% alcohol solution. The sections were placed in 0.01 mol/L sodium citrate buffer (pH = 6.0), heated to boiling in a microwave oven, and the process repeated three times for 5min each time. After permeabilizing the sections with 3% hydrogen peroxide 0.1% Triton X-100 for 30 min, the sections were blocked with 5% bovine serum albumin (BSA) solution for 1 h, then add the primary antibody diluent (rat-anti-Nestin; mouse anti-NeuN; mouse anti-synapsin-1 (SYN-1); mouse anti-Aβ<sub>1-42</sub>, all diluted 200 times, Millipore, Billerica, MA, United States) at 4°C overnight. Then add Cy3-or HRP- labeled secondary antibody diluent (1:250, Jackson ImmunoResearch Lab, West Grove, PA, United States) in the dark for 60 min at room temperature. 4, 6-diamidino-2-phenylindole (DAPI, Sigma-Aldrich, St. Louis, MO, United States) or DAB chromogenic solution was added to each section for 5–15 min, respectively. After washing with PBS, add an anti-fluorescence quencher to mount the slides, observe and take pictures under a fluorescence microscope. As it does in the previous reports (Li H. et al., 2021; Xiao et al., 2021), we use ImageJ software to scan the fluorescence intensity of each field to measure the expression level.

## Enzyme-linked immunosorbent assays

The mouse brain tissue was added to cold normal saline (NS) to prepare 10% homogenates and then centrifuged for 10 min at 3,000/min. The levels of synaptophysin (SYP), postsynaptic density-95 (PSD-95), interleukin-6 (IL-6), IL-1β and tumor necrosis factor-α (TNF-α) in the supernatant were evaluated by ELISA kit (Wuhan Elite Biotechnology Co., Ltd. Wuhan, China) according to the kit instructions. Add 100 μL of supernatant to a 96-well plate and incubate at 37°C for 90 min. 100 μL biotinylated antibody working solution was added immediately after discarding the liquid and then incubated at 37°C for 60 min. Discard the liquid and wash 3 times, then add horseradish peroxidase-conjugated (HRP, Genview, United States) enzyme conjugate working solution 100 μL to each well, incubate at 37°C for 30 min, and then discard the liquid and wash 5 times. Add 90 μL of substrate solution to each well in

dark conditions and incubate at 37°C for 15 min. The absorbance of each well at 450 nm was detected using a microplate spectrophotometer immediately after adding 50 µL of stop solution.

## Hematoxylin and eosin and nissl staining

To evaluate the morphological changes of neurons and brain damage in mice, H&E and Nissl staining were performed as previously described (Su et al., 2019; Wang et al., 2019). Briefly, brain sections were dehydrated by 70%, 80%, and 90% alcohol solution and then stained with hematoxylin. Put the slices into 1% hydrochloric acid alcohol solution to fade until the color turns red. After being washed until the color returned blue, the sections incubated with 0.5% ammonia hydroxide and followed by dying with eosin for 5 s, permeabilized with dimethylbenzene after dehydration, and then sealed with neutral gum. For Nissl staining, the brain sections were stained with Cresyl violet after being degreased with different concentrations of alcohol solution (Xiao et al., 2021).

## Terminal deoxynucleotidyl transferase dUTP nick end labeling assay

TUNEL assay can detect apoptotic DNA strand breaks in cell nuclei. The above brain sections were fixed with 4% paraformaldehyde and then permeabilized with 0.1% Triton X-100. After being washed with PBS, they were incubated with PE buffer for 1 h at 37°C and counterstained the nuclear with DAPI. Use an inverted fluorescence microscope to take pictures of brain sections and use ImageJ software to count the TUNEL-positive cells.

## Metabolomics analysis

Using Ultimate 3,000 liquid chromatograph (LC) combined with Q Exactive mass spectrometer (MS, Thermo), we performed metabolomics to investigate the mechanism by which BLWE ameliorates cognitive impairment by promoting nerve regeneration in APP/PS1 mice. A portion of mouse brain tissue is stored at -80°C for 24 h. After thawing, accurately weighed 50 mg and homogenized with 80% cold aqueous methanol 800 µL for 90 s, then vortex and shake to mix well. Ultrasonic extraction at 4°C for 30 min, stand at -20°C for 1 h, vortex for 30 s, and then stand at 4°C for 0.5 h. After centrifugation (4°C, 12,000 rpm, 15 min), transfer all supernatant to a new centrifuge tube and let them stand at -20°C for 1 h, then centrifuged again under the above conditions. Pipette 200 µL of the supernatant, add 5 µL of internal standard dichlorophenylalanine (140 µg/mL) and transfer to a sample vial for LC-MS analysis.

The chromatographic column for LC-MS is ACQUITY UPLC HSS T3 column (100 mm × 2.1 mm × 1.8 µm) and was

carried out in positive ion mode. The column temperature was 40°C, and a flow rate of 0.3 ml/min was used in this study. 0.05% formic acid aqueous solution and acetonitrile solution were used as mobile phase A and mobile phase B, respectively. Inject 4 µL sample at the injection temperature of 4°C for determination. The heater temperature of MS was 300°C, following 45 arb sheath gas flow rate, 15 arb auxiliary gas flow rate, and 1arb exhaust gas flow rate. The electrospray voltage and capillary temperatures were 3.0 KV and 350°C, respectively.

The original data underwent peak alignment, retention time correction, and peak area extraction. The identification of the metabolite structure adopts accurate mass matching (<30 ppm) and secondary spectrum matching and searches the Human Metabolome Database (HMDB). Then use autoscaling or UV method to normalize the data. Use MetaboAnalysis tool suite, SIMCA-P software (Umetrics AB, Umea, Sweden), and Kyoto Encyclopedia of Genes and Genomes (KEGG) databases for multi-dimensional statistical analysis and single-dimensional statistical analysis, including principal component analysis (PCA), partial least squares discriminant analysis (PLS-DA), Students' t-test, multiple variation analysis, and pathway enrichment analysis (Ji et al., 2018).

## Western blot analysis

WB analysis was performed according to the method in the literature (Yan et al., 2017; Xiao et al., 2022). Briefly, after the brain tissue of each mouse was weighed, Lysis Buffer, a protease inhibitor, a phosphatase inhibitor, and PMSF were added in sequence according to the manufacturer's instructions (R&D, Emeryville, CA, United States) to extract the total protein. 8% SDS-PAGE was formulated to fractionate the protein and then transferred it onto PVDF membranes. After transfer, the PVDF membrane was washed with TBST and then blocked with 5% BSA. The membrane was probed with primary antibodies for 18 h at 4°C as follows: rabbit polyclonal antibody against t-GSK-3β, t-β-catenin, p-β-catenin (1:1000, Cell signaling, United States), mouse polyclonal antibody against p-Tyr216-GSK-3β, CyclinD<sub>1</sub> and GAPDH (1:1000, Santa Cruz, United States). After washing three times, the membrane was put into HRP-labeled anti-rabbit or anti-mouse secondary antibodies and incubated at room temperature for 1 h. The proteins were visualized with Electrochemiluminescence (ECL) WB detection reagents (Millipore, Billerica, MA, United States) and then analyzed using ImageJ software.

## Statistical analysis

All experiments were repeated at least 3 times, and data were expressed as means ± SD. The differences among multiple groups were analysed by one-way analysis of variance (ANOVA)

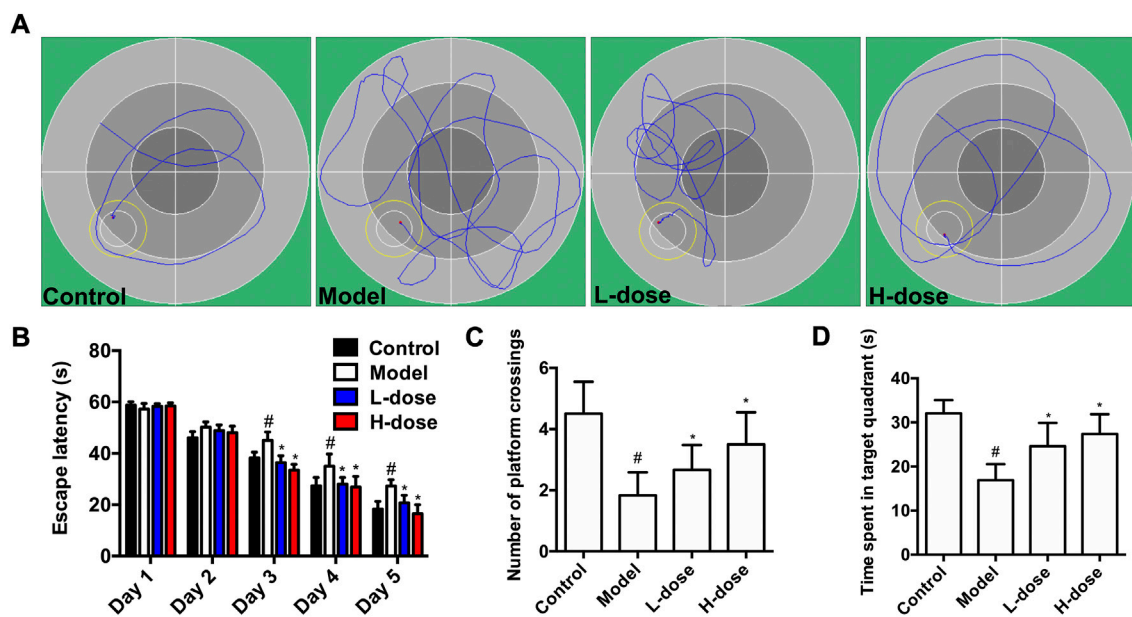


FIGURE 1

BLWE improved learning and memory ability in APP/PS1 mice. Representative individual swimming trajectory diagram in the water maze trial of each group (at day 5) (A). Comparison of escape latency in different groups of mice in place navigation test (B). Comparison of the number of platform crossings in each group in the space exploration experiment (C). Comparison of the time spent in target quadrant of each group in the space exploration experiment (D). # $p < 0.05$  vs. the control group; \* $p < 0.05$  vs. the model group. Values were expressed as the mean  $\pm$  SD ( $n = 6$  per group).

followed by Tukey's post-hoc test. The statistical significance between the two groups was analysed by two-way ANOVA followed by Bonferroni post-hoc test. The above analysis was performed using the SPSS version 13.0 statistics software, and  $p < 0.05$  was considered statistically significant.

## Results

### BLWE improved cognitive impairment in APP/PS1 mice

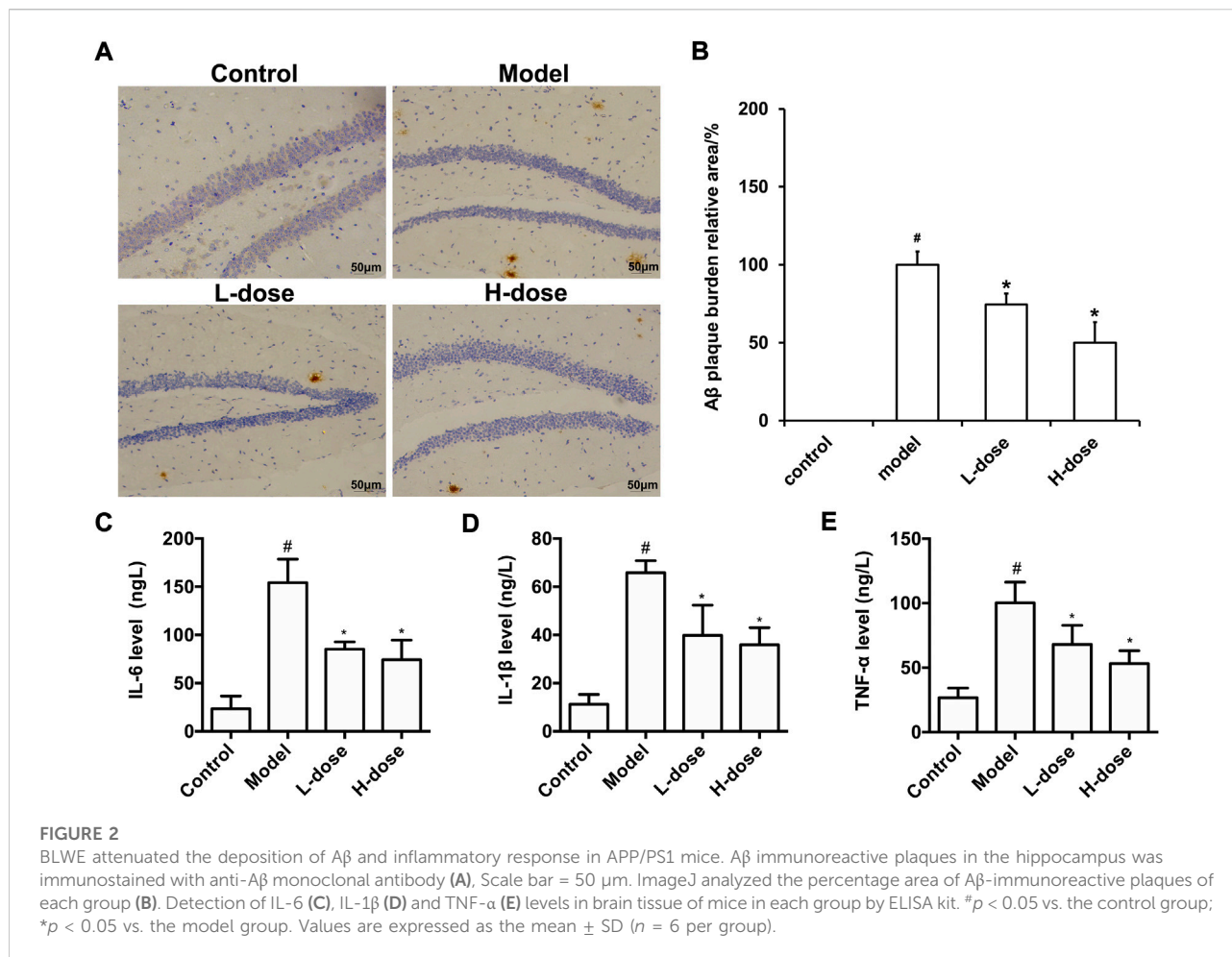
A water maze test was first performed to explore the improvement effect of BLWE on the learning and memory abilities of AD mice. The representative swimming trajectory diagram of each group is shown in Figure 1A. The place navigation test results showed that, with the extension of training time, the escape latency of mice in each group gradually shortened, and there were clearly differences among each group after 4 days of training. At day 5, the mice in the control group had the shortest escape latency at 18.32 s, while those in the model group had the longest escape latency at 27.33 s, and there was a significant difference between the two groups ( $p < 0.05$ , Figure 1B). Meanwhile, after the mice were treated with low and high doses of BLWE, their escape latency

was significantly shortened to 20.85 s and 16.57 s compared with the model group, respectively ( $p < 0.05$ , Figure 1B).

Subsequently, the spatial probe test was performed to detect the maintenance of memory function. As shown in Figure 1C, the average number of platform crossings in the model group was 1.83, significantly different from that in the control group ( $p < 0.05$ ). However, the average number of platform crossings was increased considerably after BLWE treatment (2.67 in the BLWE L-dose group and 3.50 in the BLWE H-dose group); both were statistically significant compared with the model group ( $p < 0.05$ ). In addition, the swimming times of mice in the target quadrant in the BLWE group were significantly prolonged than that in the model group (16.90 s in the model group vs. 24.62 s in the BLWE L-dose group and 27.40 s in the BLWE H-dose group,  $p < 0.05$ , Figure 1D). The above results indicated that BLWE treatment could enhance both the learning and memory function of APP/PS1 mice.

### BLWE attenuated the deposition of A $\beta$ and inflammatory response in APP/PS1 mice

After the MWM test, immunohistochemistry stained the A $\beta$  burden in the brains of mice in each group. The results revealed that there was no A $\beta$  plaque deposition in the control group,



while obvious brownish-yellow deposition of A $\beta$  plaques of different sizes and diffusely distributed could be observed in the brain of the model group (Figure 2A). Compared with the model group, BLWE treatment significantly reduced the A $\beta$  plaque positive area in the brain, which was the most significant reduction in the BLWE H-dose group (Figure 2B,  $p$  < 0.05).

The abnormal deposition of A $\beta$  can activate microglia in the brain, thus promoting the release of inflammatory factors, such as TNF- $\alpha$ , IL-1 $\beta$ , and IL-6. The released inflammatory factors will cause inflammation response in the brain, accelerate the formation of senile plaques due to nerve fiber tangles, and further worsen the course of AD. In order to evaluate the effect of BLWE on the inflammatory reaction in the brain of AD mice, the levels of IL-6, IL-1 $\beta$ , and TNF- $\alpha$  in the whole brain tissue were analyzed by an ELISA kit. The results exhibited that the levels of IL-6, IL-1 $\beta$ , and TNF- $\alpha$  were increased significantly in the brain of the model group, and after BLWE treatment, the levels of these inflammatory factors were significantly reduced, indicating that BLWE can inhibit the inflammatory reaction in the brain (Figures 2C–E,  $p$  < 0.05).

## BLWE promoted endogenous NSCs proliferation and increased the number of newborn neurons in APP/PS1 mice

Proliferating NSCs were labeled with Nestin<sup>+</sup>/BrdU<sup>+</sup> to test and verify the effect of BLWE on neurogenesis. As shown in Figure 3A,B, the Nestin<sup>+</sup>/BrdU<sup>+</sup> cells in the model group were only  $12.00 \pm 2.61$ , which was significantly reduced compared with  $21.67 \pm 3.01$  in the control group ( $p$  < 0.05). At the same time, we observed that both BLWE L-dose and H-dose treatment can significantly increase the number of Nestin<sup>+</sup>/BrdU<sup>+</sup> cells in the brains of AD mice ( $16.83 \pm 2.71$  cells in the L-dose group and  $18.50 \pm 2.88$  cells in the H-dose group vs. the model group,  $p$  < 0.05). These results indicate that BLWE can enhance the proliferation of endogenous NSCs in APP/PS1 mouse brains.

Next, we further explored whether BLWE treatment can increase the number of newborn neurons in APP/PS1 mice. Immunostaining against NeuN was used to label neurons, and BrdU was used to label proliferative cells. It can be observed in Figure 3C,D significantly fewer NeuN<sup>+</sup>/BrdU<sup>+</sup> cells were detected in the model group ( $14.33 \pm 5.32$  cells) than that in the control

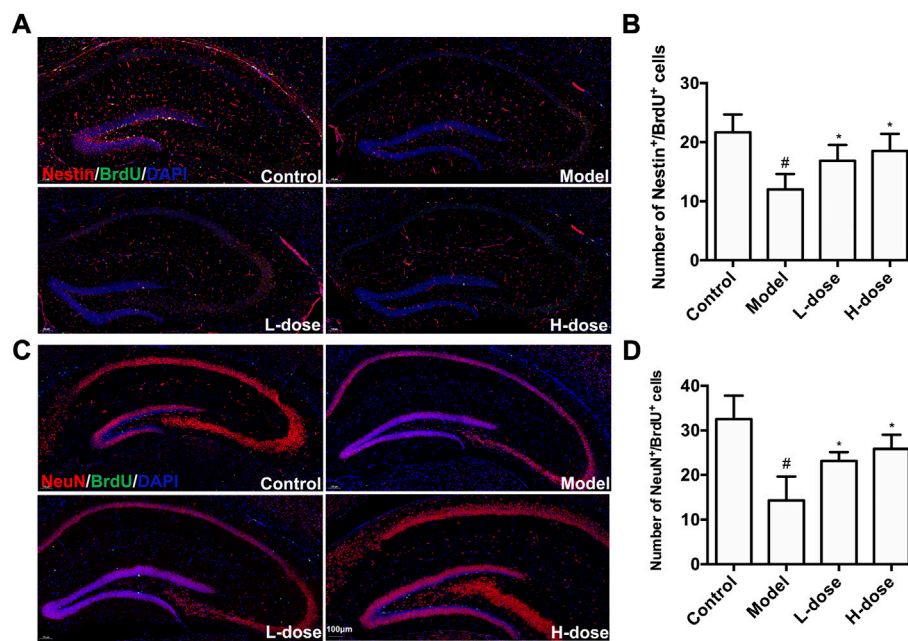


**FIGURE 3**

BLWE enhanced endogenous NSCs proliferation and differentiates into neurons in APP/PS1 mice. Mice were treated with different dose of BLWE or deionized water for 6 weeks and were injected with BrdU twice a day to label proliferative cells. Proliferating NSCs were labeled with antibodies against Nestin (red) and BrdU (green), respectively (A). ImageJ software counted Nestin/BrdU positive cells in each group (B). Newborn neurons were labeled with antibodies against NeuN (red) and BrdU (green), respectively (C). ImageJ software counted NeuN/BrdU positive cells in each group (D). The nucleus is counterstained with DAPI (blue). Scale bar = 100  $\mu$ m in A and C. <sup>#</sup> $p < 0.05$  vs. the control group; <sup>\*</sup> $p < 0.05$  vs. the model group. Values are expressed as the mean  $\pm$  SD ( $n = 6$  per group).

group ( $32.50 \pm 5.22$ ,  $p < 0.05$ ). In contrast, in both BLWE L-dose and BLWE H-dose groups, the number of NeuN<sup>+</sup>/BrdU<sup>+</sup> cells increased significantly ( $14.33 \pm 5.32$  cells in the model group vs.  $23.17 \pm 1.94$  cells in the BLWE L-dose group and  $25.83 \pm 3.19$  cells in the BLWE H-dose group,  $p < 0.05$ ). These findings indicated that BLWE treatments promote the proliferating NSCs differentiating into new neurons in the brain of APP/PS1 mice.

### BLWE increased the expression of synapse-associated protein in APP/PS1 mice

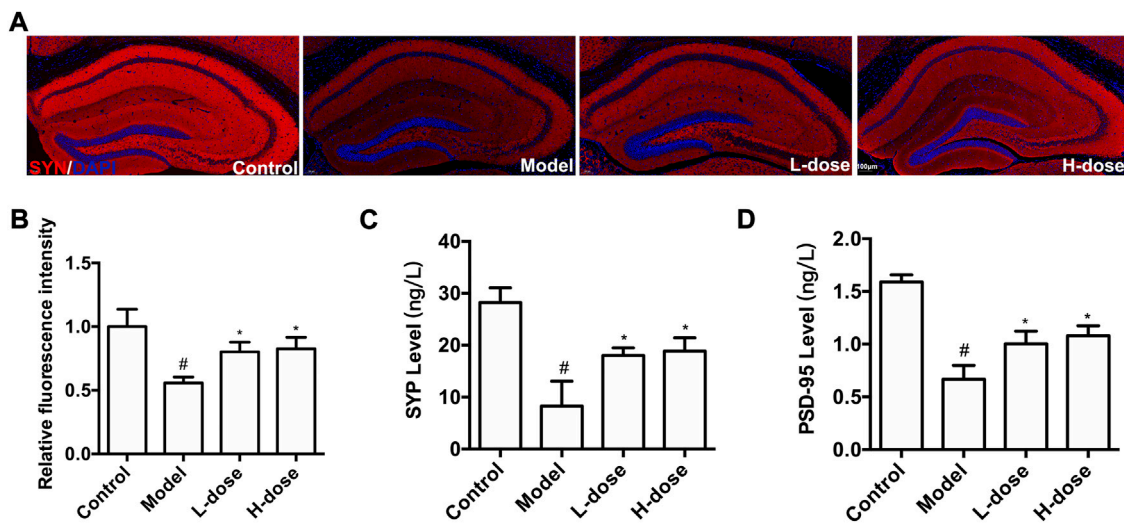
Furthermore, to determine whether new neurons can establish synaptic connections, we used immunostaining and ELISA methods to detect three important protein markers, including SYN-1, SYP, and PSD-95, which were associated with regulating synaptic plasticity and synaptic transmission (Luo et al., 2019; Muhammad et al., 2019). The fluorescence of SYN-1 in each group was shown in Figure 4A, and the expression was quantitatively analyzed using ImageJ software. Compared with the control group, the SYN-1 protein expression was significantly reduced in the model group ( $p < 0.05$ ,

Figure 4B). Nonetheless, BLWE therapy effectively restored the expression of the SYN-1 protein ( $p < 0.05$  vs. the model group, Figure 4B).

Subsequently, ELISA method was used to detect the level of PSD-95 and SYP. Results in our study demonstrated that compared with the control group, these two proteins significantly decreased in the model group ( $p < 0.05$ , Figure 4C,D), which could be reversed significantly by BLWE treatment ( $p < 0.05$ , vs. the model group, Figure 4C,D). These results indicate that BLWE can improve the expression of synapse-related proteins, which is beneficial to the repair of nerve function.

### BLWE inhibited neuron pathological damage and neuronal apoptosis in APP/PS1 mice

We used H&E, Nissl staining, and TUNEL assays to detect neuron pathological damage and apoptosis. In the control group, H&E staining revealed no significant neuronal pathological damage in the hippocampus, DG, and CA1 regions. In contrast, the model group has shrunken neurons, condensed nuclei, and blood cell congestion. Even while neuronal



**FIGURE 4** BLWE up-regulated the expression of synapse-associated proteins in APP/PS1 mice. Immunocytochemistry staining for SYN-1 (red) and DAPI (blue) in the brain of each group (A). Scale bar = 100  $\mu$ m. Quantification of the SYN-1 immunofluorescence intensity by ImageJ software (B). Quantification the concentration of SYP (C) and PSD-95 (D) by ELISA kit. #*p* < 0.05 vs. the control group; \**p* < 0.05 vs. the model group. Values are expressed as the mean  $\pm$  SD (*n* = 6 per group).

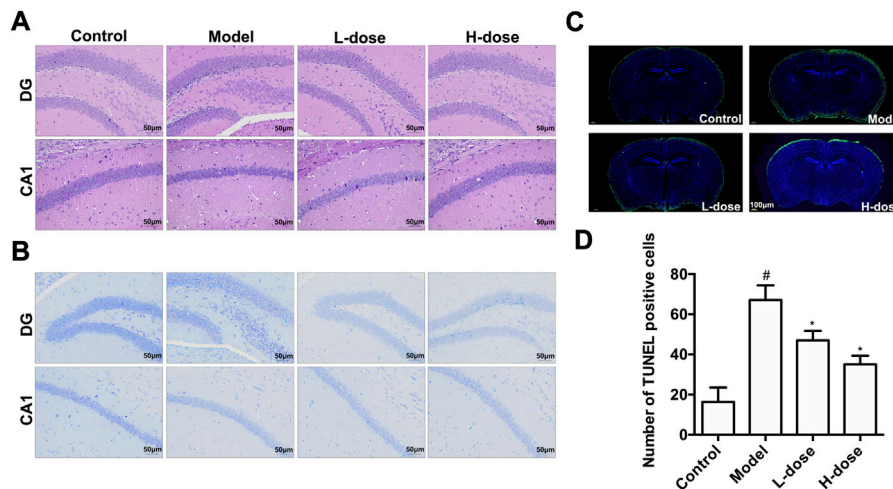
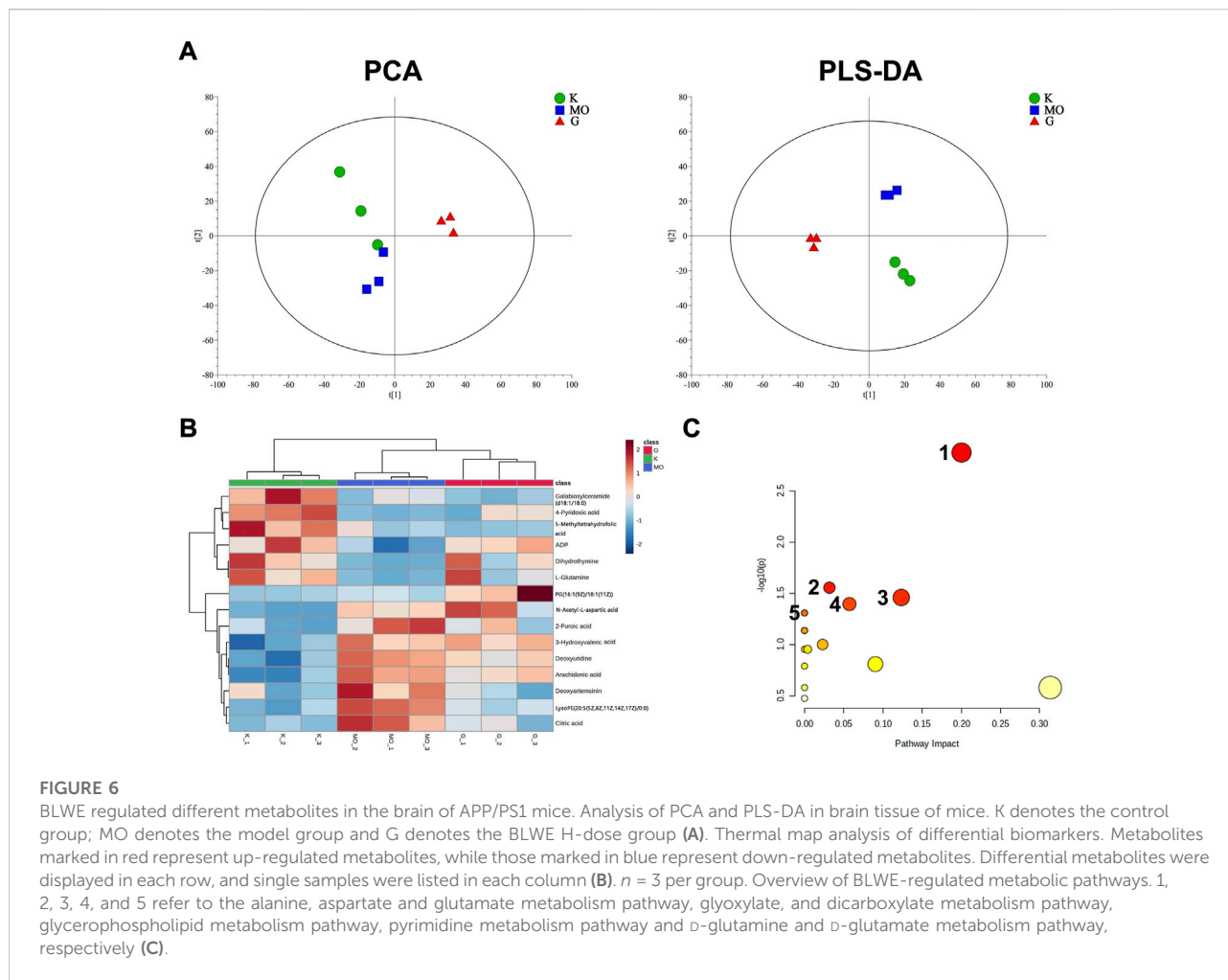


**FIGURE 5** BLWE reversed neuron pathological damage and neuronal apoptosis in APP/PS1 mice. H&E staining of hippocampus DG and CA1 areas (A). Scale bar = 50  $\mu$ m. Nissl staining of hippocampus DG and CA1 areas (B). Scale bar = 50  $\mu$ m. TUNEL staining of hippocampus DG and CA1 areas (C). Scale bar = 100  $\mu$ m. ImageJ software for quantitative counting of apoptotic cells (D). #*p* < 0.05 vs. the control group; \**p* < 0.05 vs. the model group. Values are expressed as the mean  $\pm$  SD (*n* = 6 per group).

pathological damage was also observed in the two BLWE-treated groups, it was less severe than in the model group (Figure 5A). Nissl staining was subsequently conducted to elucidate the extent of neuron loss in the brain of APP/PS1 mice. The results indicated that in the control group, the hippocampus, DG,

and CA1 area cells were neatly arranged, and the Nissl bodies were tigroid or dotted, while the Nissl bodies in the model group were blurred and the cell bodies were shrunken. After treatment with different doses of BLWE, a significant improvement in cell morphology can be observed (Figure 5B).





Moreover, we utilized the TUNEL assay to explore the improvement of neuronal apoptosis by BLWE. As shown in Figure 5C, the green fluorescent staining is TUNEL positive cells. Using ImageJ quantitative analysis, it was shown that the number of TUNEL-positive cells in the control group was only  $16.33 \pm 2.20$  cells, while it was significantly increased to  $67.17 \pm 7.25$  cells in the model group ( $p < 0.05$ , Figure 5D). Nevertheless, the number of TUNEL-positive cells was decreased in the two BLWE groups ( $47.01 \pm 4.77$  cells in the BLWE L-dose group and  $35.08 \pm 4.34$  cells in the BLWE H-dose group), which were significantly different from the model group ( $p < 0.05$ , Figure 5D), indicating that BLWE could extenuate neuronal apoptosis in APP/PS1 mice.

## Metabolomics analysis of BLWE in AD treatment

Metabolomics analysis was performed to illustrate the mechanism of anti-AD of BLWE. The results of PCA and

PLS-DA analysis showed that the samples of each group have high aggregation, and the three groups K (control group), MO (model group), and G (the BLWE H-dose group), can be distinguished by the PLS-DA analysis (Figure 6A). The control group, model group, and BLWE H-dose group can be basically divided, indicating that there are certain differences in metabolism among the three groups. As shown in Table 1, 13 different compounds were screened by KEGG database. Subsequently, the heat map results showed that the metabolites in the brain tissue of mice had significant changes after BLWE treatment. Compared with the model group, eight metabolites, including N-acetyl-aspartate (NAA), glutamine, lactosceramide, 4-pyridoxic acid, 5-methyltetrahydrofolic acid, ADP, dihydrothymine, and phosphatidylglycerol were increased, and five metabolites including citric acid, 2-furoic acid, deoxyuridine, arachidonic acid, and phosphatidylethanolamine were decreased (Figure 6B). Using the MetaboAnalyst 3.0 software, we conducted an in-depth analysis of the 13 differentially identified compounds to screen out the compounds that are related to the pathogenesis

TABLE 1 Differential metabolites screen by KEGG.

	M1.VIP [5]	M/Z	HMDB	Name	KEGG ID
1	1.54186	192.02678	HMDB0000094	Citric acid	C00158
2	1.4793	174.0396	HMDB0000812	N-Acetyl-L-aspartic acid	C01042
3	1.47922	182.0449	HMDB0000017	4-Pyridoxic acid	C00847
4	1.30564	745.50262	HMDB0010574	Phosphatidylglycerol	C00344
5	1.44032	303.2327	HMDB0001043	Arachidonic acid	C00219
6	1.44016	227.0665	HMDB0000012	Deoxyuridine	C00526
7	1.39829	145.0606	HMDB0000641	L-Glutamine	C00064
8	1.35857	127.05	HMDB0000079	Dihydrothymine	C00906
9	1.34534	458.1668	HMDB0001396	5-Methyltetrahydrofolic acid	C00440
10	1.32724	888.6236	HMDB0004866	lactosylceramide	C01290
11	1.46154	498.26245	HMDB0005779	Phosphatidylethanolamine	C00350
12	1.29828	111.0074	HMDB0000617	2-Furoic acid	C01546
13	1.2915	426.0218	HMDB0001341	ADP	C00008

of AD and that BLWE can regulate. Results showed that there were 14 metabolic pathways that BLWE might regulate. Sorted according to the degree of correlation, the top five influences were Alanine, aspartate and glutamate metabolism, Glyoxylate and dicarboxylate metabolism, Glycerophospholipid metabolism, Pyrimidine metabolism, D-glutamine and D-glutamate metabolism (Figure 6C).

To further screen the most likely intervening signaling pathways of BLWE, we imported the differential metabolites into the KEGG database for query, matching, and finally found that the affected signaling pathways included Wnt, MAPK, RAS, etc. The Wnt signaling pathway might be the most relevant pathway for BLWE treatment of AD, as most differential biomarkers were associated with it.

## BLWE enhanced neurogenesis in a Wnt signaling-dependent way

It is generally accepted that the activation of the Wnt/ $\beta$ -catenin signaling pathway affects neurogenesis (Kriska et al., 2021). To further investigate the mechanism of BLWE promoting neurogenesis in the treatment of AD, we analyzed the expression of proteins such as t-GSK-3 $\beta$ , p-Tyr216-GSK-3 $\beta$ , t- $\beta$ -catenin, p- $\beta$ -catenin, and CyclinD<sub>1</sub>, which were related to the Wnt/ $\beta$ -catenin signaling pathway (Figure 7A,B). Results showed that compared with the control group, the expression of p-Tyr216-GSK-3 $\beta$ , p-Tyr216-GSK-3 $\beta$ /t-GSK-3 $\beta$ , p- $\beta$ -catenin, and p- $\beta$ -catenin/t- $\beta$ -catenin were markedly increased, while the expression of CyclinD<sub>1</sub> was decreased in the model group ( $p < 0.001$ , Figure 7B). However, the expression of these above proteins can be reversed by BLWE treatment in which

the levels of p-Tyr216-GSK-3 $\beta$ , p-Tyr216-GSK-3 $\beta$ /t-GSK-3 $\beta$ , p- $\beta$ -catenin, and p- $\beta$ -catenin/t- $\beta$ -catenin were all down-regulated except the CyclinD<sub>1</sub> level that was up-regulated significantly ( $p < 0.01$ ,  $p < 0.05$ , Figure 7B). In addition, there was no significant difference in the protein expression of t-GSK-3 $\beta$  and t- $\beta$ -catenin among all groups. From the above results, we could conclude that BLWE enhanced neurogenesis through the Wnt/ $\beta$ -catenin signaling pathway.

## Discussion

Combined with pharmacological and metabolomics technology, this study examined the effects and molecular mechanism of BLWE in promoting endogenous NSCs proliferation and regenerative repair for AD treatment. Results confirmed that BLWE treatment for 6 weeks could activate endogenous NSCs proliferation, promote their differentiation into neurons, and establish synaptic networks, as well as reduce neuron pathological damage and neuronal apoptosis in the hippocampus, thereby enhancing the cognitive function of AD mice.

AD is a complex neurodegenerative disease characterized by A $\beta$  deposits, high tau protein phosphorylation, and neurofibrillary tangles in the cerebral cortex and hippocampus. The persistent inflammation and oxidative stress damage around the brain lesion lead to a large number of neuronal ulcerations and losses. The patient exhibited memory loss, cognitive and behavioral disorders, and eventually lost self-care abilities. At present, therapeutic drugs for AD can only compensate for the neurotransmitter that is lacking due to the loss of a large number of neurons but cannot directly supplement

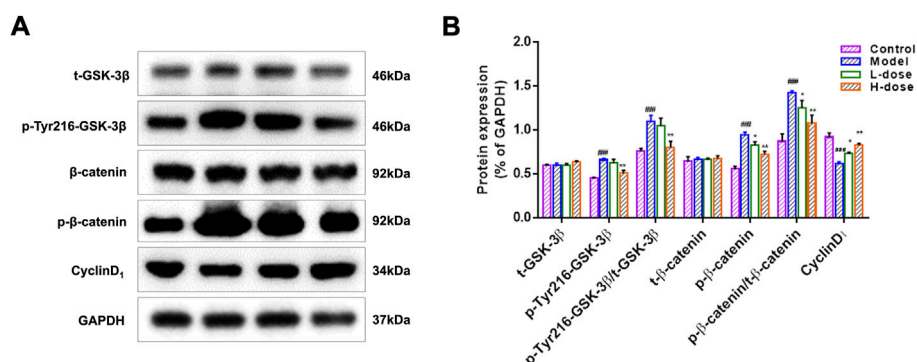


**FIGURE 7**

BLWE activated the expression of Wnt/ $\beta$ -catenin signaling pathway-associated proteins in APP/PS1 mice. Protein expression of t-GSK-3 $\beta$ , p-Tyr216-GSK-3 $\beta$ , t- $\beta$ -catenin, and p- $\beta$ -catenin in the mice brain measured by WB. GAPDH served as control (A). ImageJ software to quantify protein expression and normalized with GAPDH internal control (B). ### $p < 0.001$  vs. the control group; \* $p < 0.05$ , \*\* $p < 0.01$  vs. the model group. Values are expressed as the mean  $\pm$  SD ( $n = 6$  per group).

the neuron. Therefore, they can only partially alleviate the symptoms of mild and moderate AD patients and have serious side effects, which cannot fundamentally control the natural course of AD (Schott et al., 2019). Most mammals, including humans, have NSCs survive in the subventricular zone (SVZ) and the subgranular zone (SGZ) throughout their lives. After proliferation, the NSCs in the SGZ migrate to the granular layer of the hippocampus, and ulnar gyrus, differentiate into mature neurons and integrate their functions into the neural circuit, thereby making up for the missing neurons in the lesion. This is essential for maintaining the normal function of the hippocampus, such as the learning and memory functions (Gage, 2019; Ou et al., 2022).

We first performed MWM tests to determine the cognitive function in mice. The results indicated that the 6-week treatment of BLWE could shorten the escape latency, increase the number of plate crossings, and prolong the swimming time in the target quadrant to enhance the cognitive function of AD mice (Figures 1A–D). Secondly, we detected  $A\beta_{1-42}$  burden to explore whether BLWE can improve the typical pathological features of AD mice and found that  $A\beta_{1-42}$  deposition in the brains of mice treated with BLWE was significantly reduced (Figure 2). Further, we separately detected the number of Nestin<sup>+</sup>/BrdU<sup>+</sup> and NeuN<sup>+</sup>/BrdU<sup>+</sup> cells, the expression of synapse-related proteins to determine whether neurogenesis increases after treating with BLWE. Results show that, compared to the model group, the number of Nestin<sup>+</sup>/BrdU<sup>+</sup> and NeuN<sup>+</sup>/BrdU<sup>+</sup> cells increased significantly in the BLWE group (Figures 3A–D), indicating that BLWE could facilitate the proliferation of endogenous NSCs in the brains of AD mice and promote them to differentiate into neurons. In the process of neuron development, the formation of synaptic connections is the basis for the function of the CNS and a key step for the

development of memory. SYN-1 and SYP are specific proteins located in the presynaptic membrane, which are mainly responsible for regulating the release of neurotransmitters in synaptic vesicles, thereby participating in the transmission of chemical information. PSD-95 is the main scaffold protein located in the post-protruding membrane and plays an important role in the synaptic structure and functional plasticity, and then participates in the stability and development of the synapse (Liu et al., 2018; Royero et al., 2020; Yang et al., 2022). Our results also showed the levels of SYN-1, SYP, and PSD-95 in the model group were down regulated, while BLWE could up-regulate the level of the above synaptic proteins (Figure 4). It demonstrated that BLWE could improve synaptic plasticity, which was one of the reasons why it enhanced the cognitive function of AD mice. More importantly, through the results of H&E, Nissl, and TUNEL staining, we found that BLWE can significantly reduce the neuropathological damage caused by AD, as well as reduce neuronal cell necrosis and apoptosis (Figures 5A–D). In summary, the above experimental results were strong evidence to prove that BLWE promotes neurogenesis, thereby treating AD.

Using metabolomics technology to identify differential metabolites and analyze the metabolic pathways has important guiding significance for exploring the drug's mechanism. Gong et al. (2015) found and identified 19 biomarkers in AD model mice induced by intracerebral injection of  $A\beta_{1-42}$  by UHPLC-TOF/MS method, including proline, valine, tryptophan, LPC, plant sphingosine, and fatty acids, etc. Some scholars found that the metabolism of NAA, choline and inositol in the brain tissue of AD patients differs from that of healthy patients, and the results have certain specificity (Glodzik et al., 2015; Lin et al., 2018; Kirov et al., 2021). In our study, we used the LC-MS method to analyze the brain tissue of mice and found

13 metabolites were changed significantly, including NAA, glutamine, lactosceramide, 4-pyridoxic acid, 5-methyltetrahydrofolic acid, ADP, dihydrothymine, and phosphatidylglycerol, etc. NAA is mainly concentrated in neurons, and its decrease usually represents neurons' loss, injury, and functional defects. Most studies revealed an increase in NAA in the treatment of AD with cholinesterase inhibitors (Paslakis et al., 2014). Glutamine is the most abundant amino acid in cerebrospinal fluid and is essential for a variety of central nervous system processes, such as depression, pain, and cognitive function. Studies indicate that a drastically decreased glutamine level in the brain may be one of the diagnostic criteria for early AD patients. (Huang et al., 2017). Our research also revealed that the changes of these two important metabolites in the brains of AD mice are similar to those of AD patients. More importantly, these two metabolites can be significantly up-regulated after treatment with BLWE, which may be the main reason for improving neurological function.

By analyzing different metabolites, we determined the metabolic pathways that BLWE might affect, and then used the KEGG database to identify the signaling pathways that may also be influenced. Our results show that the Wnt signaling pathway is the most relevant to the effect of BLWE in the treatment of AD patients. The canonical Wnt signaling pathway was considered closely related to the occurrence, development, and deterioration of neurodegenerative diseases such as AD and PD (Tapia-Rojas and Inestrosa, 2018; Wu et al., 2018). Notably, neurogenesis in the hippocampus was significantly reduced when Wnt signaling was blocked (Casse et al., 2018). In the Wnt/ $\beta$ -catenin pathway,  $\beta$ -catenin is an important cytoplasmic central effector, and GSK-3 $\beta$  is an important negative regulator which could participate in the phosphorylation of  $\beta$ -catenin. Tyr216 is the excitatory phosphorylation site of GSK-3 $\beta$  protein. When the expression of p-Tyr216-GSK-3 $\beta$  decreases, the activity of GSK-3 $\beta$  is inhibited, which can inhibit the phosphorylation of  $\beta$ -catenin, hence increasing the activity of  $\beta$ -catenin, augment the transduction of Wnt signal and then initiate the transcription of downstream CyclinD<sub>1</sub> (Zeng et al., 2019). CyclinD<sub>1</sub> is one of the important factors downstream of the Wnt/ $\beta$ -catenin signaling pathway, which is related to the process of neurodegenerative diseases such as AD and PD. Researches have shown that activating the Wnt/ $\beta$ -catenin signaling pathway can initiate CyclinD<sub>1</sub> transcription, and the increased expression of CyclinD<sub>1</sub> can promote the activation of the pathway (Liu et al., 2021). Our results found that the expression of p-Tyr216-GSK-3 $\beta$  and p- $\beta$ -catenin, the ratio of p-Tyr216-GSK-3 $\beta$ /GSK-3 $\beta$  and p- $\beta$ -catenin/ $\beta$ -catenin in the brain of AD mice all increased significantly. However, these proteins were significantly downregulated by BLWE. These results indicated that the GSK-3 $\beta$  protein was activated, and the transduction of the

Wnt signal was weakened in AD mice but can be reversed by BLWE treatment. Meanwhile, we also found that the expression of CyclinD<sub>1</sub> protein was decreased significantly in the AD mice but increased after BLWE treatment. CyclinD<sub>1</sub>, a regulator of cyclin dependent kinases (CDKs), plays an important role in promoting cell proliferation and is a key molecule in regulating neurons from G<sub>0</sub> to G<sub>1</sub>. Current study suggested that the therapeutic effect of BLWE in promoting neurogenesis in the treatment of AD may be achieved by initiating CyclinD<sub>1</sub> transcription and then activating the Wnt/ $\beta$ -catenin signaling pathway.

In addition, we also focused on the astrocyte-mediated glutamate-glutamine cycle (GGC), which can support the metabolic demands and neurotransmitter transmission of neurons, promote the establishment of synaptic connections between neurons and form neural networks (Tani et al., 2014; Sidoryk-Wegrzynowicz and Struzynska, 2019). NAA and glutamine are precisely the key substances in GGC. Based on this, we speculate that the BLWE can promote neurogenesis, and treatment of AD may also be related to astrocytes, which will be the key point to our further research in the future.

## Conclusion

The present study evaluated the effects of BLWE in promoting neurogenesis in the treatment of AD and used metabolomics technology to screen different metabolites, and then accurately analyzed its mechanism. BLWE can promote the regeneration of neurons in the brain and establish synaptic connections. These effects may be achieved by activating the Wnt/ $\beta$ -catenin signaling pathway. These findings provide an experimental foundation for the application of BLWE in TCM clinical treatment of AD.

## Data availability statement

The original contributions presented in the study are included in the article/Supplementary Material, further inquiries can be directed to the corresponding author.

## Ethics statement

The animal study was reviewed and approved by the Experimental Animal Ethics Committee of Jiangsu Food & Pharmaceutical Science College.

## Author contributions

Study design: Y-HY, Q-PX; Data collection: Y-HY, Y-WS, Z-HH, and YJ; Analysis and interpretation: Y-HY, S-YL, and

B-WY; Statistical analysis: M-YZ and LS; Drafting manuscript: Y-HY and Q-PX; Revision manuscript: Y-HY and Y-WS. All authors read and approved the final manuscript.

## Funding

This work was supported by the National Natural Science Foundation of China (grant number 82104422); Natural Science Foundation of Huai'an City (Grant numbers HAB201915, HAB202067); Natural Science Foundation of the Universities of Jiangsu Province (grant numbers 21KJA360006, 20KJA360007, and 21KJB360012); High-end Training Program for Teacher Professional Leaders in Higher Vocational Colleges in Jiangsu Province (Grant number 2022TDFX004); and "Huai Shang Elite" project [grant number (2020)19].

## References

- Casse, F., Richetin, K., and Toni, N. (2018). Astrocytes' contribution to adult neurogenesis in physiology and alzheimer's disease. *Front. Cell. Neurosci.* 12, 432. doi:10.3389/fncel.2018.00432
- Chen, X., Chen, H. S., Peng, C., and Shen, J. G. (2019b). Active compounds and molecular targets of Chinese herbal medicine for neurogenesis in stroke treatment: Implication for cross talk between Traditional Chinese Medicine and biomedical sciences. *World J. Tradit. Chin. Med.* 5, 104–115. doi:10.4103/wjtcn.wjtcn\_14\_19
- Chen, X., Wu, H., Chen, H., Wang, Q., Xie, X. J., and Shen, J. (2019a). Astragaloside VI promotes neural stem cell proliferation and enhances neurological function recovery in transient cerebral ischemic injury via activating EGFR/MAPK signaling Cascades. *Mol. Neurobiol.* 56 (4), 3053–3067. doi:10.1007/s12035-018-1294-3
- de Almeida, E. J. R., Ibrahim, H. J., Chitolina Schetinger, M. R., de Andrade, C. M., and Cardoso, A. M. (2022). Modulation of inflammatory mediators and microglial activation through physical exercise in alzheimer's and Parkinson's diseases. *Neurochem. Res.* 47, 3221–3240. doi:10.1007/s11064-022-03713-x
- Gage, F. H. (2019). Adult neurogenesis in mammals. *Science* 364 (6443), 827–828. doi:10.1126/science.aav6885
- Glodzik, L., Sollberger, M., Gass, A., Gokhale, A., Rusinek, H., Babb, J. S., et al. (2015). Global N-acetylaspartate in normal subjects, mild cognitive impairment and Alzheimer's disease patients. *J. Alzheimers Dis.* 43 (3), 939–947. doi:10.3233/JAD-140609
- Golde, T. E., DeKosky, S. T., and Galasko, D. (2018). Alzheimer's disease: The right drug, the right time. *Science* 362 (6420), 1250–1251. doi:10.1126/science.aau0437
- Gong, Y., Liu, Y., Zhou, L., Di, X., Li, W., Li, Q., et al. (2015). A UHPLC-TOF/MS method based metabonomic study of total ginsenosides effects on Alzheimer disease mouse model. *J. Pharm. Biomed. Anal.* 115, 174–182. doi:10.1016/j.jpba.2015.07.007
- Hanspal, M. A., and Gillotin, S. (2022). A new age in understanding adult hippocampal neurogenesis in Alzheimer's disease. *Neural Regen. Res.* 17 (12), 2615–2618. doi:10.4103/1673-5374.339472
- Huang, D., Liu, D., Yin, J., Qian, T., Shrestha, S., and Ni, H. (2017). Erratum to: Glutamate-glutamine and GABA in brain of normal aged and patients with cognitive impairment. *Eur. Radiol.* 27 (7), 2706–2707. doi:10.1007/s00330-017-4753-8
- Jaberi, R., Mirsadeghi, S., and Kiani, S. (2021). *In vitro* characterization of subventricular zone isolated neural stem cells, from adult monkey and rat brain. *Mol. Biol. Rep.* 48 (2), 1311–1321. doi:10.1007/s11033-021-06201-7
- Ji, H., Liu, Y., He, F., An, R., and Du, Z. (2018). LC-MS based urinary metabolomics study of the intervention effect of aloe-emodin on hyperlipidemia rats. *J. Pharm. Biomed. Anal.* 156, 104–115. doi:10.1016/j.jpba.2018.04.015
- KirovII, Sollberger, M., Davitz, M. S., Glodzik, L., Soher, B. J., Babb, J. S., et al. (2021). Global brain volume and N-acetyl-aspartate decline over seven decades of

## Conflict of interest

The authors declare that the research was conducted in the absence of any commercial or financial relationships that could be construed as a potential conflict of interest.

## Publisher's note

All claims expressed in this article are solely those of the authors and do not necessarily represent those of their affiliated organizations, or those of the publisher, the editors and the reviewers. Any product that may be evaluated in this article, or claim that may be made by its manufacturer, is not guaranteed or endorsed by the publisher.

normal aging. *Neurobiol. Aging* 98, 42–51. doi:10.1016/j.neurobiolaging.2020.10.024

Kong, L., Hu, Y., Yao, Y., Jiao, Y., Li, S., and Yang, J. (2015). The Coumarin derivative osthole stimulates adult neural stem cells, promotes neurogenesis in the Hippocampus, and ameliorates cognitive impairment in APP/PS1 transgenic mice. *Biol. Pharm. Bull.* 38 (9), 1290–1301. doi:10.1248/bpb.b15-00142

Kriska, J., Janeckova, L., Kirdajova, D., Honsa, P., Knotek, T., Dzamba, D., et al. (2021). Wnt/ $\beta$ -Catenin signaling promotes differentiation of ischemia-activated adult neural stem/progenitor cells to neuronal precursors. *Front. Neurosci.* 15, 628983. doi:10.3389/fnins.2021.628983

Li, H., Lei, T., Zhang, J., Yan, Y., Wang, N., Song, C., et al. (2021a). Longan (*Dimocarpus longan* Lour.) Aril ameliorates cognitive impairment in AD mice induced by combination of D-gal/A $\beta$ 1 and an irregular diet via RAS/MEK/ERK signaling pathway. *J. Ethnopharmacol.* 267, 113612. doi:10.1016/j.jep.2020.113612

Li, Y. H., Jin, Y., Wang, X. S., Chen, X. L., Chen, H. B., Xu, J., et al. (2021b). Neuroprotective effect of fructus broussonetiae on APP/PS1 mice via upregulation of AKT/ $\beta$ -Catenin signaling. *Chin. J. Integr. Med.* 27 (2), 115–124. doi:10.1007/s11655-019-3178-4

Liang, Z., Li, X., Luo, X., Luo, H., Chen, Y., Cai, M., et al. (2022). The Aptamer Ob2, a novel AChE inhibitor, restores cognitive deficits and alleviates amyloidogenesis in 5xFAD transgenic mice. *Mol. Ther. Nucleic Acids* 28, 114–123. doi:10.1016/j.omtn.2022.02.018

Lin, R., Li, L., Zhang, Y., Huang, S., Chen, S., Shi, J., et al. (2018). Electroacupuncture ameliorate learning and memory by improving N-acetylaspartate and glutamate metabolism in APP/PS1 mice. *Biol. Res.* 51 (1), 21. doi:10.1186/s40659-018-0166-7

Liu, P., Wang, L. Y., Wang, Y. Q., Wang, R. L., Li, F. F., Zhang, S., et al. (2020). The Chinese herb Fructus Broussonetiae aids learning and memory in chronic cerebral hypoperfusion by reducing proinflammatory microglia activation in rats. *J. Integr. Neurosci.* 19 (1), 21–29. doi:10.31083/j.jin.2020.01.1213

Liu, X., Wang, K., Wei, X., Xie, T., Lv, B., Zhou, Q., et al. (2021). Interaction of NF- $\kappa$ B and wnt/ $\beta$ -catenin signaling pathways in alzheimer's disease and potential active drug treatments. *Neurochem. Res.* 46 (4), 711–731. doi:10.1007/s11064-021-03227-y

Liu, Y., Zhang, Y., Zheng, X., Fang, T., Yang, X., Luo, X., et al. (2018). Galantamine improves cognition, hippocampal inflammation, and synaptic plasticity impairments induced by lipopolysaccharide in mice. *J. Neuroinflammation* 15 (1), 112. doi:10.1186/s12974-018-1141-5

Llorens-Bobadilla, E., and Martin-Villalba, A. (2017). Adult NSC diversity and plasticity: The role of the niche. *Curr. Opin. Neurobiol.* 42, 68–74. doi:10.1016/j.conb.2016.11.008

Luo, H., Xiang, Y., Qu, X., Liu, H., Liu, C., Li, G., et al. (2019). Apelin-13 suppresses neuroinflammation against cognitive deficit in a streptozotocin-induced rat model of alzheimer's disease through activation of BDNF-TrkB signaling pathway. *Front. Pharmacol.* 10, 395. doi:10.3389/fphar.2019.00395

- Menet, R., Lecordier, S., and ElAli, A. (2020). Wnt pathway: An emerging player in vascular and traumatic mediated brain injuries. *Front. Physiol.* 11, 565667. doi:10.3389/fphys.2020.565667
- Muhammad, T., Ali, T., Ikram, M., Khan, A., Alam, S. I., and Kim, M. O. (2019). Melatonin rescue oxidative stress-mediated neuroinflammation/neurodegeneration and memory impairment in scopolamine-induced amnesia mice model. *J. Neuroimmune Pharmacol.* 14 (2), 278–294. doi:10.1007/s11481-018-9824-3
- Ou, Y., Zhou, M., Che, M., Gong, H., Wu, G., Peng, J., et al. (2022). Adult neurogenesis of the median eminence contributes to structural reconstruction and recovery of body fluid metabolism in hypothalamic self-repair after pituitary stalk lesion. *Cell. Mol. Life Sci.* 79 (8), 458. doi:10.1007/s00018-022-04457-1
- Pang, S. Q., Wang, G. Q., Lin, J. S., Diao, Y., and Xu, R. A. (2014). Cytotoxic activity of the alkaloids from *Broussonetia papyrifera* fruits. *Pharm. Biol.* 52 (10), 1315–1319. doi:10.3109/13880209.2014.891139
- Paslakis, G., Traber, F., Roberz, J., Block, W., and Jessen, F. (2014). N-acetyl-aspartate (NAA) as a correlate of pharmacological treatment in psychiatric disorders: A systematic review. *Eur. Neuropsychopharmacol.* 24 (10), 1659–1675. doi:10.1016/j.euroneuro.2014.06.004
- Royero, P. X., Higa, G. S. V., Kostecki, D. S., Dos Santos, B. A., Almeida, C., Andrade, K. A., et al. (2020). Ryanodine receptors drive neuronal loss and regulate synaptic proteins during epileptogenesis. *Exp. Neurol.* 327, 113213. doi:10.1016/j.expneurol.2020.113213
- Schott, J. M., Aisen, P. S., Cummings, J. L., Howard, R. J., and Fox, N. C. (2019). Unsuccessful trials of therapies for Alzheimer's disease. *Lancet* 393 (10166), 29. doi:10.1016/S0140-6736(18)31896-8
- Shakir, M. N., and Dugger, B. N. (2022). Advances in deep neuropathological phenotyping of alzheimer disease: Past, present, and future. *J. Neuropathol. Exp. Neurol.* 81 (1), 2–15. doi:10.1093/jnen/nlab122
- Sidoryk-Wegrzynowicz, M., and Struzynska, L. (2019). Astroglial contribution to tau-dependent neurodegeneration. *Biochem. J.* 476 (22), 3493–3504. doi:10.1042/BCJ20190506
- Su, Y. T., Guo, Y. B., Cheng, Y. P., Zhang, X., Xie, X. P., Chang, Y. M., et al. (2019). Hyperbaric oxygen treatment ameliorates hearing loss and auditory cortex injury in noise exposed mice by repressing local Ceramide accumulation. *Int. J. Mol. Sci.* 20 (19), E4675. doi:10.3390/ijms20194675
- Sun, S., Zhu, X. J., Huang, H., Guo, W., Tang, T., Xie, B., et al. (2019). WNT signaling represses astrogliogenesis via Ngn2-dependent direct suppression of astrocyte gene expression. *Glia* 67 (7), 1333–1343. doi:10.1002/glia.23608
- Tani, H., Dulla, C. G., Farzampour, Z., Taylor-Weiner, A., Huguenard, J. R., and Reimer, R. J. (2014). A local glutamate-glutamine cycle sustains synaptic excitatory transmitter release. *Neuron* 81 (4), 888–900. doi:10.1016/j.neuron.2013.12.026
- Tapia-Rojas, C., and Inestrosa, N. C. (2018). Loss of canonical Wnt signaling is involved in the pathogenesis of Alzheimer's disease. *Neural Regen. Res.* 13 (10), 1705–1710. doi:10.4103/1673-5374.238606
- Uddin, M. S., Kabir, M. T., Tewari, D., Mamun, A. A., Mathew, B., Aleya, L., et al. (2020). Revisiting the role of brain and peripheral A $\beta$  in the pathogenesis of Alzheimer's disease. *J. Neurol. Sci.* 416, 116974. doi:10.1016/j.jns.2020.116974
- Wang, L., Song, L. F., Chen, X. Y., Ma, Y. L., Suo, J. F., Shi, J. H., et al. (2019). MiR-181b inhibits P38/JNK signaling pathway to attenuate autophagy and apoptosis in juvenile rats with kainic acid-induced epilepsy via targeting TLR4. *CNS Neurosci. Ther.* 25 (1), 112–122. doi:10.1111/cns.12991
- Wu, D. M., Han, X. R., Wen, X., Wang, S., Fan, S. H., Zhuang, J., et al. (2018). Salidroside protection against oxidative stress injury through the wnt/ $\beta$ -catenin signaling pathway in rats with Parkinson's disease. *Cell. Physiol. Biochem.* 46 (5), 1793–1806. doi:10.1159/000489365
- Xiao, H. H., Chen, J. C., Li, H., Li, R. H., Wang, H. B., Song, H. P., et al. (2022). Icarisid II rescues cognitive dysfunction via activation of Wnt/ $\beta$ -catenin signaling pathway promoting hippocampal neurogenesis in APP/PS1 transgenic mice. *Phytother. Res.* 36 (5), 2095–2108. doi:10.1002/ptr.7430
- Xiao, H., Wang, Y., Wu, Y., Li, H., Liang, X., Lin, Y., et al. (2021). Osthole ameliorates cognitive impairments via augmenting neuronal population in APP/PS1 transgenic mice. *Neurosci. Res.* 164, 33–45. doi:10.1016/j.neures.2020.04.001
- Yan, Y. H., Li, S. H., Li, H. Y., Lin, Y., and Yang, J. X. (2017). Osthole protects bone marrow-derived neural stem cells from oxidative damage through PI3K/Akt-1 pathway. *Neurochem. Res.* 42 (2), 398–405. doi:10.1007/s11064-016-2082-y
- Yan, Y., Kong, L., Xia, Y., Liang, W., Wang, L., Song, J., et al. (2018). Osthole promotes endogenous neural stem cell proliferation and improved neurological function through Notch signaling pathway in mice acute mechanical brain injury. *Brain Behav. Immun.* 67, 118–129. doi:10.1016/j.bbi.2017.08.011
- Yang, G. Z., Gao, Q. C., Li, W. R., Cai, H. Y., Zhao, H. M., Wang, J. J., et al. (2022). (D-Ser2) oxyntomodulin recovers hippocampal synaptic structure and theta rhythm in Alzheimer's disease transgenic mice. *Neural Regen. Res.* 17 (9), 2072–2078. doi:10.4103/1673-5374.335168
- Yu, N., Zhu, K. J., Ma, S. J., Tang, H., and Tan, X. N. (2017). The total flavonoids of *Clerodendrum bungei* suppress A549 cells proliferation, migration, and invasion by impacting Wnt/ $\beta$ -Catenin signaling. *World J. Tradit. Chin. Med.* 3, 15–20. doi:10.4103/wjtc.wjtc\_18\_17
- Zeng, Q., Long, Z., Feng, M., Zhao, Y., Luo, S., Wang, K., et al. (2019). Valproic acid stimulates hippocampal neurogenesis via activating the wnt/ $\beta$ -catenin signaling pathway in the APP/PS1/nestin-GFP triple transgenic mouse model of alzheimer's disease. *Front. Aging Neurosci.* 11, 62. doi:10.3389/fnagi.2019.00062
- Zhang, H., Su, Y., Sun, Z., Chen, M., Han, Y., Li, Y., et al. (2021). Ginsenoside Rg1 alleviates A $\beta$  deposition by inhibiting NADPH oxidase 2 activation in APP/PS1 mice. *J. Ginseng Res.* 45 (6), 665–675. doi:10.1016/j.jgr.2021.03.003
- Zhang, Y., Biao, Y., Chu, X., Hao, L., Shi, C., Liu, Y., et al. (2020). Protective effect of Chushizi (*Fructus Broussonetiae*) on acetaminophen-induced rat hepatitis by inhibiting the Toll-like receptor 3/c-Jun N-terminal kinase/c-jun/c-fos/janus protein tyrosine kinase/activators of transcription 3 pathway. *J. Tradit. Chin. Med.* 40 (6), 965–973. doi:10.19852/j.cnki.jtcm.2020.06.008

## Glossary

**AD** Alzheimer's disease

**A $\beta$**  amyloid beta peptide

**NMDA** N-methyl-D-aspartic acid

**AchE** acetylcholinesterase

**NSCs** neural stem cells

**CNS** central nervous system

**APP/PS1** amyloid beta precursor protein/presenilin-1

**Tg** transgenic

**BL** *Broussonetia papyrifera* (L.) L'Hér. ex Vent. fruits

**BLWE** *Broussonetia papyrifera* (L.) L'Hér. ex Vent. fruits water extract

**GSK-3 $\beta$**  glycogen synthase kinase-3 $\beta$

**BrdU** 5-Bromo-2-deoxyuridine

**MWM** Morris water maze

**NeuN** neuronal nuclei

**BSA** bovine serum albumin

**SYN** synapsin

**SYP** synaptophysin

**PSD-95** postsynaptic density protein 95

**ELISA** Enzyme-linked immunosorbent assay

**SDS** sodium dodecyl sulfate

**H&E** hematoxylin and eosin

**PBS** phosphate buffered saline

**TUNEL** terminal deoxynucleotidyl transferase dUTP nick end labeling

**DAPI** 4,6-diamidino-2-phenylindole

**NS** normal saline

**HRP** horseradish peroxidase conjugated

**ECL** electrochemiluminescence

**LC** liquid chromatograph

**MS** mass spectrometer

**PVDF** polyvinylidene fluoride

**HMDB** Human Metabolome Database

**KEGG** Kyoto Encyclopedia of Genes and Genomes

**PCA** principal component analysis

**PLS-DA** partial least squares discriminant analysis

**OPLS-DA** orthogonal partial least squares

**SVZ** subventricular zone

**SGZ** subgranular zone

**TCM** Traditional Chinese medicine.